11th World Congress on Structural and Multidisciplinary Optimisation
07th -12th, June 2015, Sydney Australia

Reliability-based design optimization of vehicle front-end structure for pedestrian lower extremity protection

Guangyong Sun[1], Xiaojiang Lv[1,2], Jianguang Fang[3], Xianguang Gu[1], Qing Li[3]

1 State Key Laboratory of Advanced Design and Manufacturing for Vehicle Body, Hunan University, Changsha, 410082, China, sgy800@126.com;
2 Zhejiang Key Laboratory of Automobile Safety Technology, Geely Automobile Research Institute, Hangzhou, 311228, China;
3 School of Aerospace, Mechanical and Mechatronic Engineering, The University of Sydney, Sydney, NSW 2006, Australia

Abstract
Injuries to the lower extremities are one of the major issues in vehicle to pedestrian collisions. To minimize injury risks of pedestrian lower extremity, this paper presents the design optimization of a typical vehicle front-end structure subjected to two different impact cases of TRL-PLI and Flex-PLI. Several approaches involving sampling techniques, surrogate model, multiobjective optimization algorithm and reliability analysis are introduced and applied. In order to take into account the effect of design variables uncertainty, the reliability-based design optimization (RBDO) is conducted, and a Monte Carlo Simulation (MCS) is adopted to generate random distributions of the constraint functions for each design. The differences of the different Pareto fronts of the deterministic optimization and RBDO are compared and analyzed in this study. Finally, the reliability-based optimum design result is verified by using test validation. It is shown that the pedestrian lower extremity injury can be substantially improved for meeting product development requirements through the proposed approach.

Keywords: Reliability optimization; Vehicle front-end structure; Pedestrian protection; Multiple impact cases

1. Introduction

According to World Health Organization (WHO) statistical data, 22% of deaths on the world roads are pedestrians, and this proportion is as high as two thirds in some countries [1]. Meanwhile, the frequency of lower extremity injuries is higher in vehicle to pedestrian collisions. For example, serious lower extremity injuries from bumper contact occurred in 43% of seriously injured pedestrian cases in US, 35% in German and 43% in Japan [2-3]. So, researches on protection of pedestrian lower extremity have become a very important part in both the academe and automotive industry.

To evaluate the performance of lower extremity protection, two different subsystem legform tests have been used in the extensive government regulations and standards. One is Transport Research Laboratory Pedestrian Legform Impactor (TRL-PLI) in the European Union (EU) regulation, the other is Flexible Pedestrian Legform Impactor (Flex-PLI) in European New Car Assessment Program (EuroNCAP) [4-5]. For instance, Shin et al. [6] performed bumper size optimization and the result could meet requirements of TRL-PLI impact. Lee et al. [7] researched the front-end structure for Flex-PLI impact. However, the above investigations on design optimization in the existing literature mainly focus on the single legform impactor. Matsui [8] investigated the characteristics of safety assessment results of different vehicle types using the TRL-PLI and the Flex-PLI. The results showed that the tibia injury assessment was different between the TRL-PLI and the Flex-PLI owing to their different sensor types. So, the vehicle front-end structure is subjected to multiple legform impactor cases which should be verified for the required regulation and standard. However, the traditional approach is to tune the design manually for each test mode separately. It is therefore hardly to find a design that is work properly for all test modes.

All optimization problems cannot neglect the uncertainty, which exists in material properties, geometries and manufacturing precision etc. In order to take into account various uncertainty, Reliability-based design optimization (RBDO) is introduced and aims at finding a reliable optimum solution by converting the deterministic constraints into probabilistic ones. Many researchers have focused on this field [9-12]. Nevertheless, vehicle front-end structural optimization for minimizing injury risks of TRL-PLI and Flex-PLI impact considering the uncertainty has received limited attention in the literature. To address the issue, The paper presents a comprehensive study approach of how different non-deterministic optimization schemes are performed in the design of vehicle front-end structure under multiple impact cases.

2 Performance assessment and experimental validation

2.1 TRL-PLI and Flex-PLI

According to EU regulation, the fracture risk of the tibia is evaluated from the upper tibia acceleration (a_{UT}) and the knee ligament damage risk is evaluated from the knee bending angle (a_{KB}) and knee shear displacement

(D_{KS}) as shown in Figure 1(a). The fracture risk of the tibia is evaluated from the tibia bending moment measured at multiple locations, and the knee ligament damage risk is evaluated from knee ligament elongations of Anterior Cruciate Ligament (ACL), Posterior Cruciate Ligament (PCL), and Medial Collateral Ligament (MCL) according to EuroNCAP as shown in Figure 1(b).

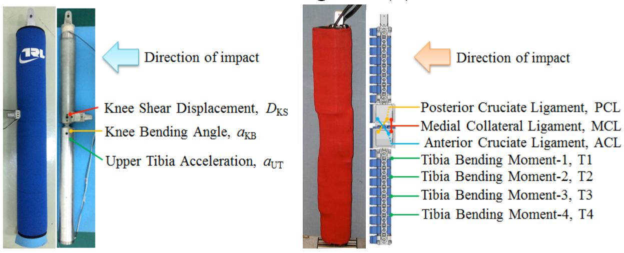

(a) TRL-PLI (b) Flex-PLI

Figure 1: Injury criteria

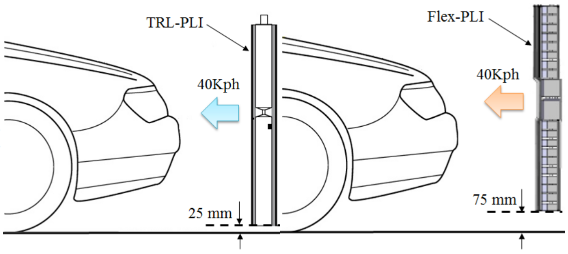

(a) TRL-PLI (b) Flex-PLI

Figure 2: The test condition of legform-to-bumper

2.2 Assessment of TRL-PLI and Flex-PLI

Tibia and knee injuries are assessed after completion of the legform-to-bumper test under the conditions shown in Figure 2. The initial velocity of two impact cases is 40 kph. In this study, the impact location is selected as the center of the bumper. The test results of the TRL-PLI and Flex-PLI injury is shown in Table 1. According to Table 1, the a_{UT} of the TRL-PLI (197.2g) is higher than the EU regulation limit value (170g). It is found that the ACL (11.2mm) is more than 10mm, which cannot meet the Euro-NCAP assessment rating requirements.

Table 1 The assessment of the TRL-PLI and Flex-PLI test results

	TRL-PLI				*Flex-PLI*			
	Injury	*Requirement*	*Test*	*Assessment*	*Injury*	*Requirement*	*Test*	*Assessment*
Tibia injuries	a_{UT} (g)	≤ 170	197.2	Violated	T1 (Nm)	≤ 282	209.1	Satisfied
					T2 (Nm)	≤ 282	264.5	Satisfied
					T3 (Nm)	≤ 282	278.3	Satisfied
					T4 (Nm)	≤ 282	161.5	Satisfied
Knee injuries	a_{KB} (°)	≤ 19	13.1	Satisfied	MCL (mm)	≤ 19	16.4	Satisfied
	D_{KS} (mm)	≤ 6	2.3	Satisfied	ACL (mm)	≤ 10	11.2	Violated
	/	/	/	/	PCL (mm)	≤ 10	5.0	Satisfied

To meet the design requirement, the multiobjective reliability-based optimization design is introduced to design the front-end structure for minimize injury values of TRL-PLI and Flex-PLI. This procedure is shown in Figure 3. The Optimal Latin Hypercube Sampling (OLHS) technique adopted for constructing the surrogate models. The RBF model is constructed based on the response results of sampling points. The MOPSO is applied to search the optimal solution set. The Monte Carlo Simulation (MCS) is applied to perform a reliable analysis.

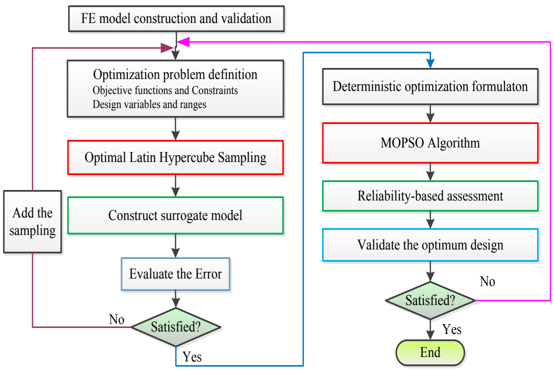

Figure 3: Flowchart of the reliability design optimization process

2.3 Numerical model and validation

To assess the protection performance of various vehicle front-end structures, the finite element (FE) model need be constructed. The baseline model, as shown in Figure 4, consists of the following groups of components: bumper, hood, front rail, lamp, energy absorbing plate, spoiler support plate et al. In this study, the validity of CAE model is conducted by comparing the simulation results with the corresponding physical test results with these curves of a_{UT} and ACL elongation as plotted in Figure 5. From which, the simulation curves of the a_{UT} and ACL elongation all well agree with the corresponding results obtained from the physical test. The maximum difference between simulation and test is less than 5% and the total area and trend of curves are rather alike. As shown in Figure 6, each legform campaign gesture agrees well with the physical test. Therefore, the CAE model is accurate and effective for the vehicle front-end structure design optimization in the subsequent study.

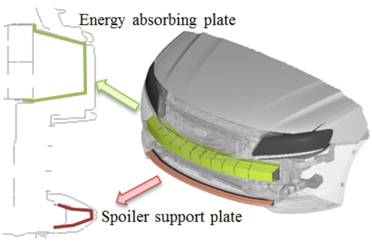

Figure 4: The FE model

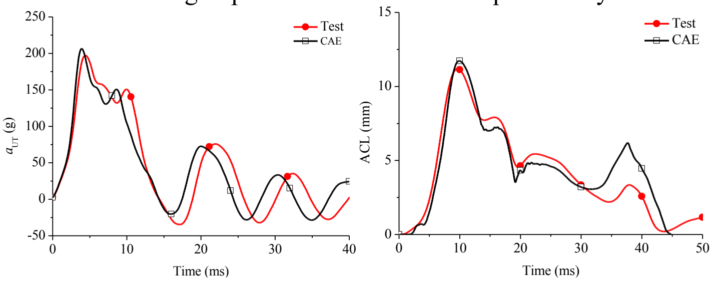

Figure 5: Comparison of the curves between simulation and physical test

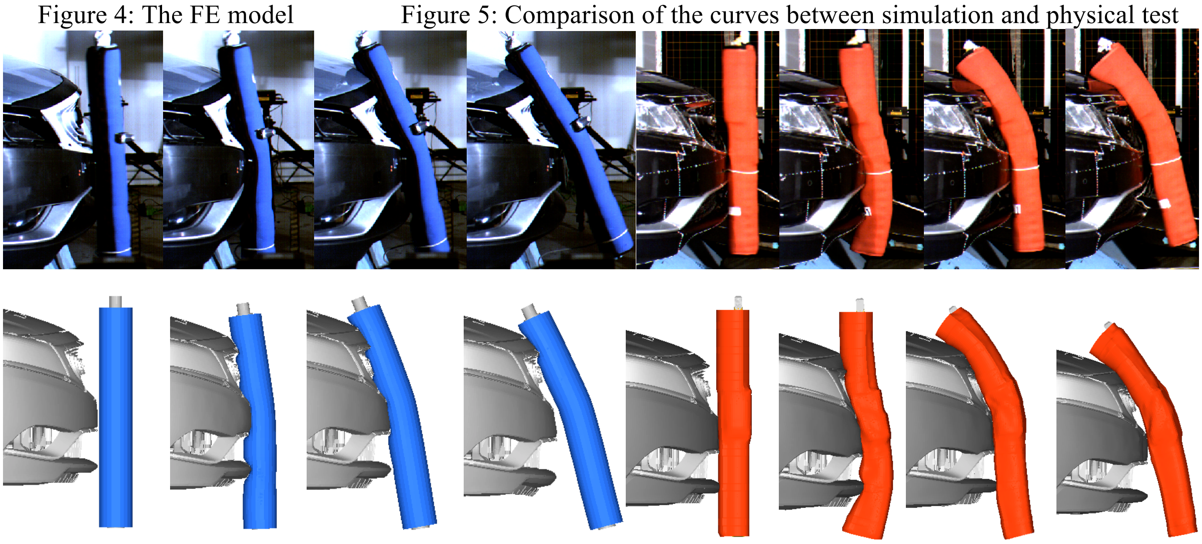

0ms 10ms 20ms 30ms 0ms 10ms 20ms 30ms

(a) TRL-PLI (b) Flex-PLI

Figure 6: Different time steps of TRL-PLI and Flex-PLI impact between the simulation and physical test

3 Vehicle front-end structure design optimization

3.1 Design responses and variables

From engineering experience, the rigidity of energy absorbing plate and spoiler support plate have important effect on pedestrian legform injury, thereby making the best possible combination of these components under each legform impact conditions. The thickness of energy absorbing plate (x_1), the X-direction distance of energy absorbing plate (x_2), the thickness of spoiler support plate (x_3), the X-direction distance of spoiler support plate (x_4), have significant influences on front-end structure rigidity. Thus, these parameters are taken as design variables, as show in Figure 7. Table 2 provides the list of the design variables, the baseline design values, as well as the corresponding lower and upper bounds. In order to take into account the uncertainties, the design variables are assumed to distribute normally in this study, whose coefficient of variation is given as 5% from typical manufacturing and assembly tolerance. The variations of design parameters are selected in terms of possible design changes allowed.

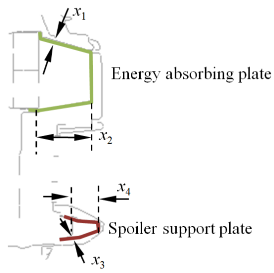

Figure 7: Design variables

According to Table 1, the upper tibia acceleration of TRL-PLI and ACL of Flex-PLI could not meet the design requirements. For this reason, they are chosen as the design objectives in Table 3. Considering that the design variables have an influence on other eight injury values of TRL-PLI and Flex-PLI, and eight of them are chosen as the constraints. Table 3 lists the responses of baseline design and the allowance of each constraint.

Table 2 The value of the design variables

Design variations	*Distribution*	*COV(σ/μ)*	*Initial value*	*Boundary value*	
				Lower	*Upper*
x_1	Normal	5%	1.0mm	0.6mm	1.4mm
x_2	Normal	5%	80mm	20mm	100mm
x_3	Normal	5%	1.0mm	0.6mm	1.4mm
x_4	Normal	5%	80mm	20mm	100mm

Table 3 The baseline design and design optimization target

Responses	*Objectives*		*Constraints*							
	a_{UT}	*ACL*	a_{KB}	D_{KS}	*T1*	*T2*	*T3*	*T4*	*MCL*	*PCL*
	$f_1(x)$	$f_2(x)$	$g_1(x)$	$g_2(x)$	$g_3(x)$	$g_4(x)$	$g_5(x)$	$g_6(x)$	$g_7(x)$	$g_8(x)$
Baseline	206.71	11.70	13.60	2.23	218.78	263.24	290.80	162.81	16.92	5.21
Target	Min	Min	≤18.05	≤5.7	≤267.9	≤267.9	≤267.9	≤267.9	≤18.05	≤9.5

3.2 Constructed metamodel

For four continuous variables $\mathbf{x} = (x_1, x_2, x_3, x_4)$, the number of levels for each variable can be selected to be 5 and a total of 25 sampling points are generated in the design space by the OLHS method. The objective and constraint values of each sampling point are obtained by using LS-DYNA version 971. Four typical basis functions of RBF including thin-plate spline, Gaussian, multiquadric and inverse multiquadric are used and their accuracies are compared. In this study, additional 10 validation points are selected to access the accuracy of these surrogates. Based on these validation points, the accuracies of basis function of RBF model can be assessed by using estimators of R^2 and RAAE. Validation results of selected error metrics for different functions of RBF metamodel are shown in Table 4. The fitting results of multiquadric function of RBF model are very good with high values of $R^2 \geq 0.9$ and low RAAE≤ 0.3. Therefore, the Multiquadric function of RBF model is considered most suitable and are selected to perform the design optimization below.

Table 4 Error assessment for different functions of RBF metamodel

	Thin-plate spline		*Gaussian*		*Multiquadric*		*Inverse multiquadric*	
	R^2	*RAAE*	*R^2*	*RAAE*	*R^2*	*RAAE*	*R^2*	*RAAE*
a_{UT}	0.9092	0.574	0.8412	0.273	0.9532	0.252	0.9462	0.331
ACL	0.8721	0.413	0.8651	0.440	0.9123	0. 231	0.9354	0.332
a_{KB}	0.8126	0.388	0.8135	0.255	0.934	0.218	0.8936	0.327
D_{KS}	0.8215	0.554	0.8341	0.465	0.9616	0.222	0.9321	0.251
T1	0.8934	0.257	0.815	0.367	0.9251	0.159	0.8955	0.359
T2	0.8232	0.452	0.8189	0.279	0.9294	0.212	0.9094	0.453
T3	0.8971	0.630	0.9063	0.312	0.9571	0.203	0.9013	0.370
T4	0.9136	0.471	0.933	0.307	0.9072	0.291	0.9036	0.271
MCL	0.8752	0.484	0.8653	0.491	0.9136	0.289	0.9022	0.284
PCL	0.8751	0.352	0.8852	0.342	0.9203	0.291	0.8713	0.451

3.3 Reliability-based design optimization

In the reliability-based design optimization, the desired reliability of eight design constraints (R_j) are set as 95% and 99%. And the minimize value of mean value is set for the two objectives, respectively. The reliability-based design is formulated as:

$$\begin{cases} \min & \mu(f_1(\mathbf{x})) \\ & \mu(f_2(\mathbf{x})) \\ s.t. & P(g_1(\mathbf{x}) \le 18.05°) \ge R_j \\ & P(g_2(\mathbf{x}) \le 5.7mm) \ge R_j \\ & P(g_3(\mathbf{x}) \le 267.9Nm) \ge R_j \\ & P(g_4(\mathbf{x}) \le 267.9Nm) \ge R_j \\ & P(g_5(\mathbf{x}) \le 267.9Nm) \ge R_j \\ & P(g_6(\mathbf{x}) \le 267.9Nm) \ge R_j \\ & P(g_7(\mathbf{x}) \le 18.05mm) \ge R_j \\ & P(g_8(\mathbf{x}) \le 9.5mm) \ge R_j \\ & \mathbf{x}^L \le \mathbf{x} \le x^U, \ \mathbf{x} = (x_1, x_2, x_3, x_4)^T \end{cases} \tag{1}$$

The four design variables according to the probability distribution defined previously are incorporated, and reliability-based optimization is performed. The Pareto fronts are obtained using the MOPSO algorithm with the population size (50) and number of generations (100). The MCS is consisted with 10,000 descriptive sampling points using given distribution in this study. Performing the Monte Carlo analysis using RBF to the functions instead of CAE function evaluations allows a significant reduction in the cost of the procedure. Figure 8 presents the Pareto fronts for multiobjective deterministic and reliable designs.

In three Pareto fronts, each point represents one solution in different cases, which indicates the trade-off between upper tibia acceleration and ACL elongation. Obviously, these two objectives strongly compete with each other: the lower upper tibia acceleration, the higher ACL elongation. It is noted that the Pareto front of the 95% reliable design is farther away from the deterministic counterpart and the 99% reliable design is farthest away from the 95% reliable design in Figure 8.

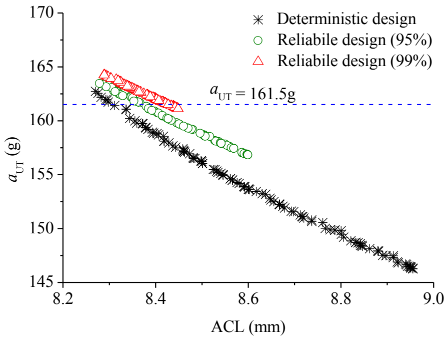

Figure 8: Pareto fronts of the deterministic and reliable design optimization

3.4 Comparison and validation of optimization results

Figure 9 shows the optimal Flex-PLI response results of physical test at different times. It is noted that the optimal is obtained by the minimum distance selection method (TMDSM). Compared with Figure 6, the third image shows that the knee bending degree is obviously abated at 20ms. The kinetic energy can be adequately absorbed by the front-end structure in the optimum design.

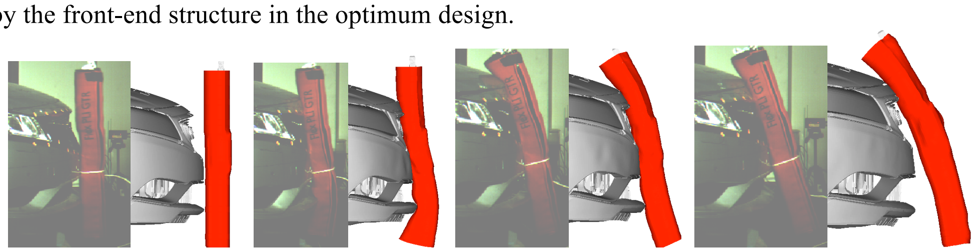

(a) 0ms (b) 10ms (c) 20ms (d) 30ms

Figure 9: Animation after the optimization design

Table 5 The test results between the baseline and optimal design

Description		*Baseline (Test)*	*Optimal result (Test)*	*Reduction (%)*
Objectives	$f_1(x)$	197.2	156.71	20.53
	$f_2(x)$	11.2	8.09	27.77
Constraints	$g_1(x)$	13.1	11.51	
	$g_2(x)$	2.3	2.38	
	$g_3(x)$	209.1	186.26	
	$g_4(x)$	264.5	252.34	

	$g_5(x)$	278.3	263.87
	$g_6(x)$	161.5	149.12
	$g_7(x)$	16.4	14.59
	$g_8(x)$	5.0	5.46
Variables	x_1	1.0mm	0.62mm
	x_2	80mm	45.02mm
	x_3	1.0mm	0.81mm
	x_4	80mm	84.98mm

According to the response values of tests, the results between the baseline and optimal is compared in Table 5. The injury values of a_{UT} and ACL elongation are reduced to 20.53% and 27.77% relative to the initial design, respectively. Thus, the optimization result satisfies the design requirements. In summary, the presented method is effective for the front-end structure design, and these results show that the optimal design has improved the pedestrian safety significantly.

4 Conclusions

A system approach has been developed to design and optimize the vehicle front-end structure for minimizing injury risks of pedestrian lower extremity based on TRL-PLI and Flex-PLI in this study. The numerical model of TRL-PLI and Flex-PLI impact vehicle was constructed first and validated with physical test. Then, the optimal Latin hypercube sampling (OLHS) method was adopted for design of experiment (DOE) and the surrogate model was constructed through Radial basis function (RBF). The optimal problems involving in a number of objectives were solved by the multiobjective particle swarm optimization (MOPSO) algorithm in this study. In order to take into account the uncertainties of design variables, the Monte Carlo simulation (MCS) is used as reliability analysis. It was found that the result of reliability-based design was more conservative than the results of deterministic optimization as expected. As the variation of performance constraint functions raised by the uncertainties of design variables was considered, the reliability of the front-end structure design for the vehicle safety was greatly improved in the real engineering application.

Acknowledgments

This work is supported jointly by National Natural Science Foundation of China (51405123, 11202072) and the Open Fund of Zhejiang Key Laboratory of Automobile Safety Technology (No. 2009E10013).

References

[1] The World Health Organization (WHO), Global status report on road safety 2013: supporting a decade of action, *WHO Report*, 2013

[2] Mallory A, Rikard F, Erik R, Bruce D, Pedestrian Injuries By Source: Serious and Disabling Injuries in US and European Cases, *Association for the Advancement of Automotive Medicine*, 56: 13-24, 2012

[3] Matsui Y, Possibility of installing a data acquisition system in a pedestrian headform impactor, *Int J Crashworthiness,* 19(2): 115-125, 2014

[4] Regulation (EC) No78/2009 of the European Parliament and of the Council of 14 January 2009, *Official J of the European Union*, 2009

[5] Euro NCAP, Pedestrian Protection Assessment Protocol, version 8.0, http://www.euroncap.com/files/, 2014

[6] M Shin, S Yi, O Kwon, G Park, Structural optimization of the automobile frontal structure for pedestrian protection and the low-speed impact test, *Proceedings of the Institution of Mechanical Engineers*, 222 (D12): 2373-2387, 2008

[7] Lee Y, Joo Y, Park J, Kim Y, Yim H, Robust design optimization of frontal structures for minimizing injury risks of flex pedestrian legform impactor, *Int J Auto Tech*, 15(5): 757-764, 2014

[8] Matsui Y, Safety assessment characteristics of pedestrian legform impactors in vehicle-front impact tests, *Accid Anal Prev,* 73: 65-72, 2014

[9] Shi L, Zhu P, Yang R, Lin S, Adaptive sampling-based RBDO method for vehicle crashworthiness design using Bayesian metric and stochastic sensitivity analysis with independent random variables, *Int J Crashworthiness*, 18(4): 331-342, 2013

[10] Gu XG, Lu JW, Wang HZ, Reliability-based design optimization for vehicle occupant protection system based on ensemble of metamodels, *Struct Multidisc Optim*, DOI 10.1007/s00158-014-1150-7, 2014

[11] Sinha K, Reliability-based multiobjective optimization for auto-motive crashworthiness and occupant safety, *Struct Multidisc Optim*, 33(3): 255-268, 2007

[12] Huang T, Wu J, Hsiao C, Wang M, Lee K, Design of a bumper system for pedestrian lower-leg protection using the Taguchi method, *J Auto Eng*, 225: 1578-1586, 2011

[13] Sun GY, Li GY, Hou SJ, Zhou SW, Li W, Li Q, Crashworthiness design for functionally graded foam-filled thin-walled structures, *Mat Sci Eng A*, 527(7-8):1911-1919, 2010